Supplementary Material

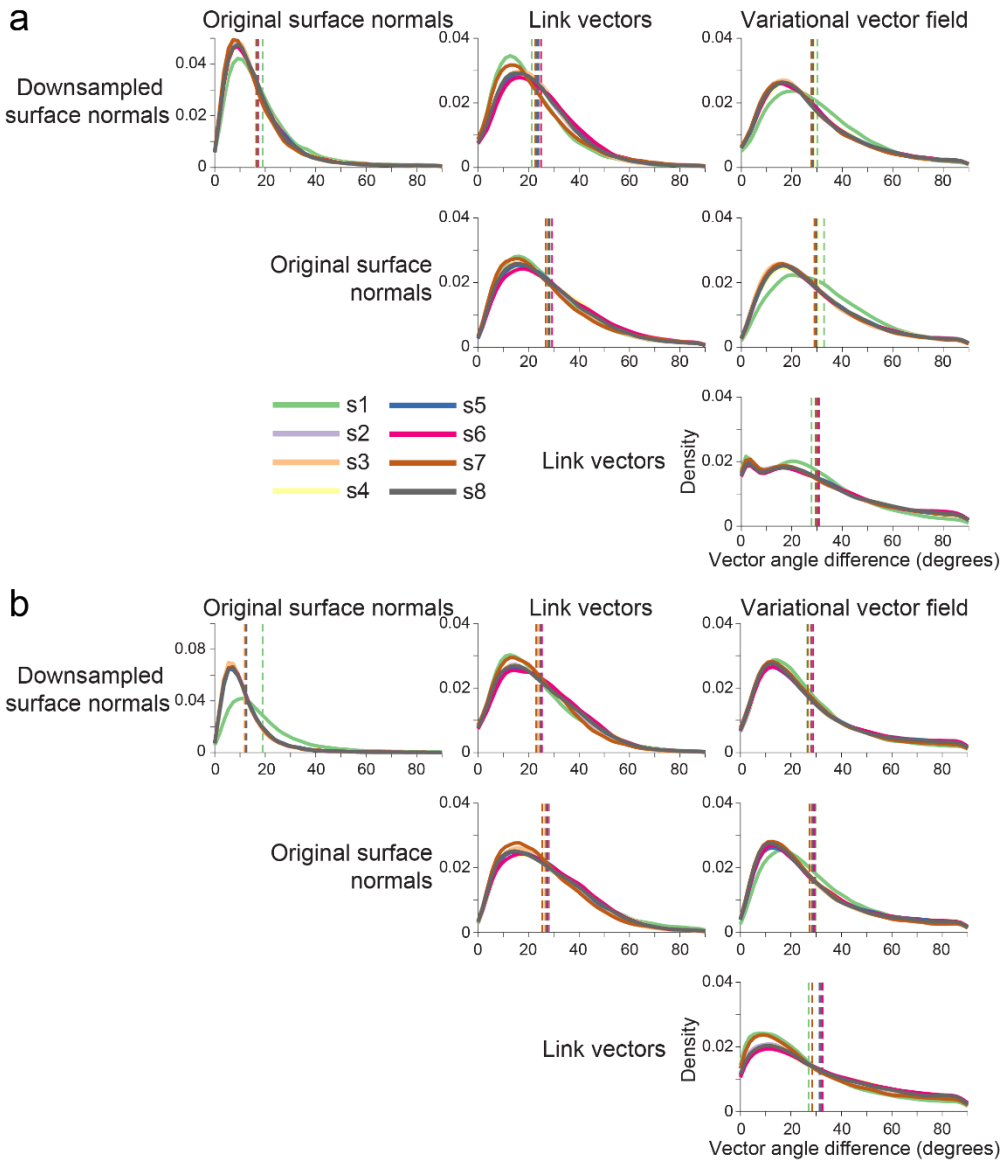

Figure S1. Dipole orientations across methods using lower resolution scans showed similar patterns of discrepancy as those obtained using high resolution scans.

a *Distribution of angular difference between dipole orientations generated using each method for each participant using pial surfaces extracted from 1mm³ T1 MRIs. Vertical dashed lines show the mean angular difference for each participant.*

b *As in (a) using white matter surfaces extracted from 1mm³ T1 MRIs.*

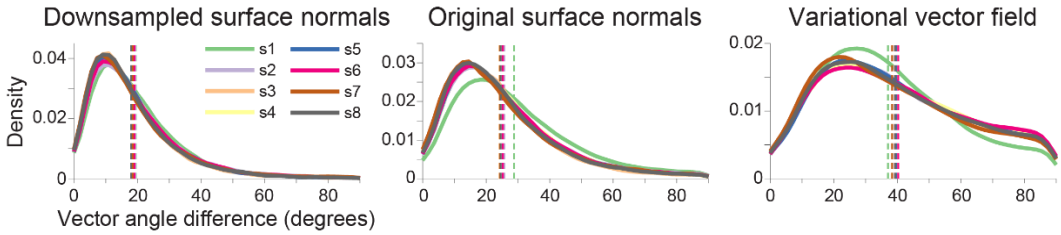

Figure S2. Substantial discrepancy in dipole orientations between pial and white matter surfaces. *Distribution of angular difference between dipole orientations at corresponding vertices on the pial and white matter surfaces, generated using the 1mm³ T1 volumes. The link vectors method is not shown because this method generates identical dipole orientations for the pial and white matter surfaces. Each solid line shows the distribution for a single participant. Vertical dashed lines show the mean angular difference for each participant.*

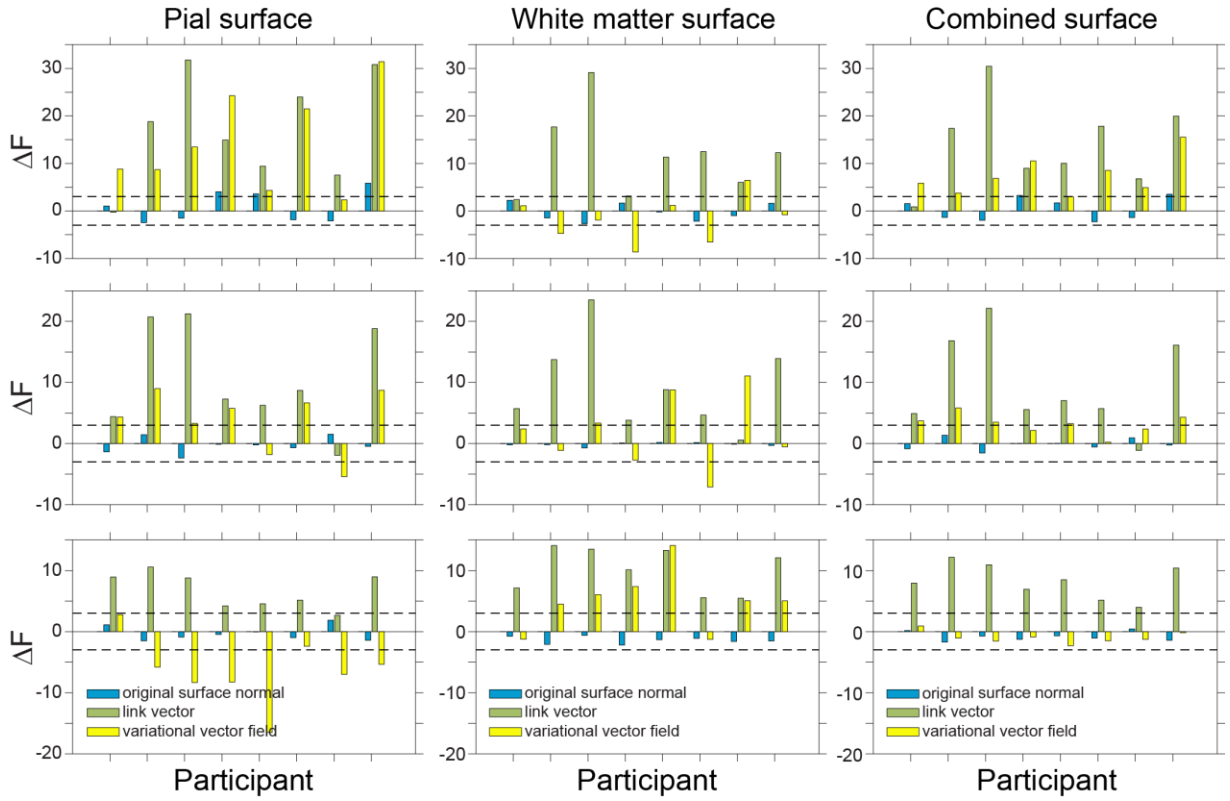

Figure S3. Results with surfaces from lower resolution scans were comparable to those obtained with high resolution surfaces. *Change in free energy (relative to the downsampled surface normals model) for each method tested for each participant for visual ERF 1 (top), visual ERF 2 (middle), and the motor ERF (bottom) using vectors derived from 1mm³ T1 volumes and source space models based on the pial (left), white matter (center), and combined pial / white matter surfaces (right).*

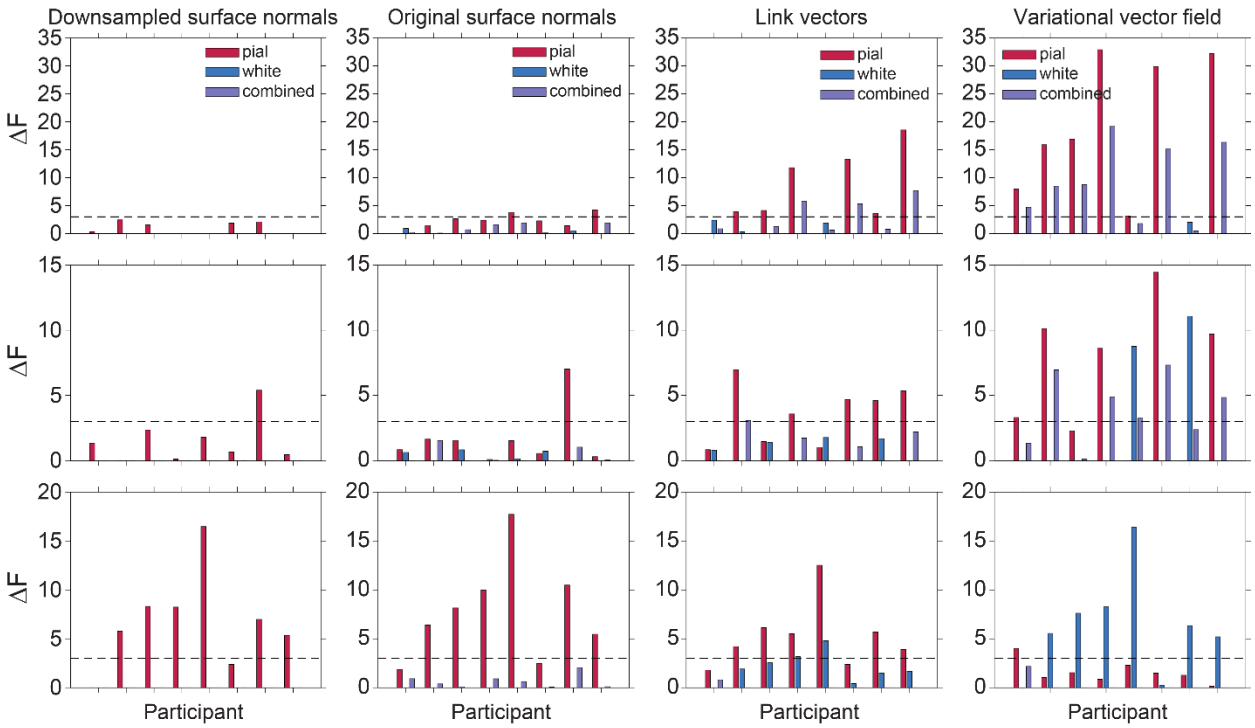

Figure S4. Results with surfaces from lower resolution scans were comparable to those obtained with high resolution surfaces. *Change in free energy (relative to the worst model) for each source space surface tested for each participant for visual ERF 1 (top), visual ERF 2 (middle), and the motor ERF (bottom) using surfaces derived from 1mm³ T1 volumes and dipole orientation vectors computed using the (from left to right), downsampled surface normals, original surface normals, link vectors, and variational vector field methods.*

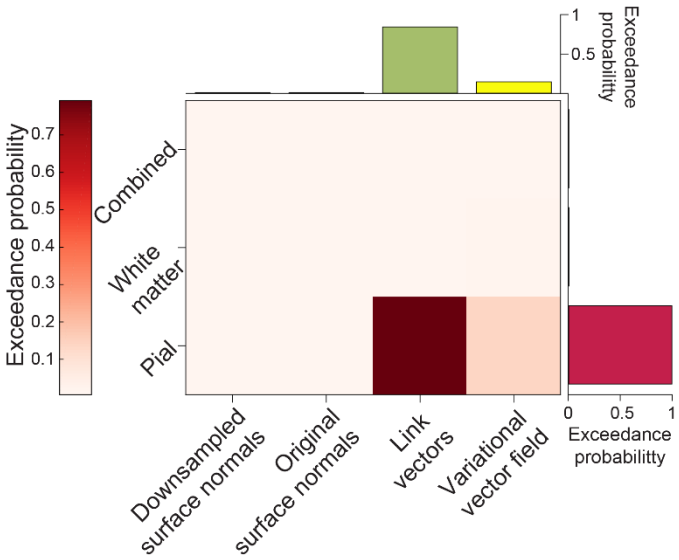

Figure S5. Source inversion using the pial surface and surface correspondence-based methods yield the best model fit overall. *Exceedance probabilities for each combination of surface (pial, white matter, and combined) and dipole orientation vector method (downsampled surface normals, original surface normals, link vectors, and variational vector field) using surfaces derived from 1mm³ MPM volumes. Top and right plots show exceedance probabilities for models grouped by surface or dipole orientation vector method alone.*